Thermal Vibration Analysis of Cracked Nanobeams Embedded in an Elastic Matrix Using Finite Element Analysis

A. I. Aria [a,1] , M. I. Friswell[b], T. Rabczuk[c,d]
[a]Tabriz University, Department of Mechanical Engineering, Tabriz, Iran.
[b]Swansea University, Bay Campus, Fabian Way, Swansea SA1 8EN, UK.
[c]Department of Civil Engineering, Bauhaus University Weimar, Weimar, Germany.
[d]Institute of Research and Development, Duy Tan University, Da Nang 550000, Vietnam.

Abstract
In this study, a finite element (FE) model is proposed to study the thermal transverse vibrations of cracked nanobeams resting on a double-parameter nonlocal elastic foundation. Hamilton's principal is employed to derive the governing equations for the free vibrations of the nanobeam. The cracked section of the beam is modelled by dividing the cracked element into two classical beam sections connected via a rotational spring positioned at the crack. The Galerkin method of weighted residuals is used to solve the equations of motion and calculate the natural frequencies. The effect of the crack length, crack position, the temperature gradient, the boundary conditions and the foundation stiffness, on the vibration response of the cracked nanobeams supported by elastic foundations is considered by including thermal effects. The FE results are compared to the available benchmark studies in the literature.

Keywords:

Cracked nanobeam; Nonlocal theory; Transverse free vibrations; Winkler-Pasternak medium; Thermal effects; Finite element.

Introduction
Recently nano/micro-structured materials have become more important due to their superior performance and because of their wide range of applications in cell manipulation [1], microsurgery [2] and micro/nano-electro mechanical systems (MEMS/NEMS) [3]. The study of micro/nano structural elements such as beams and plates at the micro/nano-length scale has attracted the attention of many researchers. Since atomic and molecular models are too expensive for design optimisation, continuum models are generally utilised in the analysis of these elements where size effects are critical [4]. High order continuum theories have received intense interest, since these theories are able to describe the size effects of micro/nano structures incorporating the interactions of non-adjacent atoms and molecules. The most popular continuum mechanics theory used to model the size effects of nanostructures is the nonlocal elasticity theory. This high order theory incorporates size effects accurately enough to model micro/nano scale structures [5]. In this theory,

[1] Corresponding author: arashimaniaria@gmail.com.

introduced by Eringen [5], the long range interactions between atoms are included. In fact, Eringen's theory assumes that the stress of a specific point in a continuum body is related to the strains at all points of that continuum, not only those near the considered point. In the recent years, many studies have analysed the vibrations and buckling of *intact* nanostructures on the basis of nonlocal elasticity [6-23]; since the list of these investigations is very long, only some of the latest studies are mentioned here. Also, in the field of electro-mechanical structures, Zhu et al, investigated the influence of the surface energy on the vibration [24] and buckling [25] behaviour of piezoelectric nano-shells. They proposed several significant methods to improve the simulated responses of piezoelectric nano-shells.

Cracks, which are common relevant defects, can decrease the stiffness of the system and consequently reduce the natural frequencies [26-34]. Since the presence of defects cannot be ignored in the fabrication of micro/nanostructures, the investigation of cracks and flaws should be considered in the design of micro/nanoelectromechanical systems. In the literature, few researchers have studied cracked nanobeams incorporating size effects. Luque et al. [35] investigated the tensile response of copper nano-wires, considering surface cracks, using molecular dynamics simulations. The transverse vibrations of cracked nanobeams were analysed by Loya et al. [36] based on Euler- Bernoulli theory with a torsional spring using nonlocal elasticity. The flexural vibration of cracked Euler–Bernoulli nanobeams considering surface effects was studied by Hasheminejad et al. [37]. By neglecting, the effect of surface density, they examined the influences of surface tension and surface elasticity. Hosseini- Hashemi et al. [38] analysed the vibration behaviour of cracked nanobeams based on surface elasticity. Using first-order shear deformation theory, they examined the influences of crack depth and location, rotary inertia, shear deformation and vibration modes. Roostai et al. [39] studied multiple cracks with various boundary conditions exploiting nonlocal elasticity theory. They utilized analytical solutions to investigate the effects of crack severity, crack location and nonlocal parameter on the fundamental frequencies of the Euler–Bernoulli nanobeam. Analysing the influences of temperature gradient and magnetic field, Karlicic et al. [40] presented an analytical model to examine the natural frequencies of a cracked Euler–Bernoulli nanobeam resting on a single parameter medium incorporating thermal effects. Tadi Beni et al. [41] studied the bending vibration of cracked nanobeam in the framework of modified coupled stress theory. They highlighted the roles of the crack location and crack severity on the bending frequency of the nanobeam. Wang and Wang [42] studied lateral vibrations of cracked nanobeams considering surface effects and using surface energy theory. Buckling and post buckling of cracked nanobeams, using the modified coupled stress theory was studied by Khorshidi et al. [43]. They modelled the microbeams by Euler Bernoulli theory with open edge cracks and studied the influence of the crack location, crack depth, and length scale parameter on microbeam's buckling and postbuckling response.

There are variety of approaches to model elastic foundations [16]. For example, Winkler's elastic medium is based on a linear spring system, which contains closely spaced linear springs. In this model, the deformation occurs only at the location where the load is applied. In the Pasternak model, shear interaction among the spring elements is modelled by connecting the ends of the springs to a structure that only undergoes bending shear deformation. In addition to these two models, there are several other methods to model the elastic medium such as the Heteny model,

the Borodicha Filonenko model, and the Kerr model. In the past few years, a range of investigations have studied the vibration and buckling behaviour of beams that are embedded in various kinds of elastic medium. Yang et al. [44] studied the free vibration of axially moving elastic beams, considering pinned-pinned boundary conditions, and supported by an elastic foundation. Murmu and Pradhan [45] examined the role of elastic foundations on the thermal free vibration of single-walled CNTs on a Winkler foundation. Amirian et al. [46] studied the shear deformation and rotatory inertia effects on the natural frequencies of single-walled CNTs. They employed first-order shear deformation theory to study the flexural vibrations of beams on Pasternak foundations. Chang [47] exploited the FE method to analyse the thermal bending vibration and pre-buckling of single-walled CNTs embedded in an elastic foundation, based on the mechanics of thermoelasticity. In order to examine linear buckling of axonal microtubules, Civalek and Demir [15] calculated the critical buckling loads for different kinds of microtubules resting on elastic foundations with various boundary conditions, using the finite element method. They also investigated thermal flexural vibrations of silicon carbides resting on a Winkler-Pasternak foundation [16] and calculated the natural frequencies for different boundary conditions.

The novelty of this study is to propose a nonlocal finite element formulation in order to investigate the thermal vibrations of cracked nanobeams that are embedded in a double-parameter elastic foundation. The governing equations are derived based on Hamilton's principle and the crack is modelled as a rotational spring. Classical beam theory is utilized and three boundary conditions are considered. In the present study, the influences of the nonlocal parameter, the crack severity, crack location, temperature and the foundation stiffness on the natural frequencies of crack nanobeams are investigated and the results are compared with previous studies available in the open literature.

2. Model Formulation

2.1 Cracked beam

A cracked beam of length l, has an edge crack of depth d_{cr} and a crack at $x = l_c$ from left (Fig. 1). It is assumed that the edge crack always remains open. The exclusion of one or more atoms in the structure of the nanobeams results in additional strain energy, that may be considered as equivalent to a crack in the continuum. The cracked nanobeam is modelled as two beams, which are connected to each other by a rotational elastic spring. This spring is assumed to include the additional strain energy, which is imposed by the existence of the crack. The increments corresponding to the strain energy with respect to the axial force and the bending moment can be given as

$$\Delta U_c = \frac{1}{2} M \Delta\theta + \frac{1}{2} N \Delta u \tag{1}$$

where $\Delta\theta$ and Δu, are the angular deformation of the rotational spring and the horizontal displacement at $x = l_c$ respectively, which are given by [36]

$$\Delta\theta = k_{MM} \frac{\partial^2 w}{\partial x^2} + k_{MN} \frac{\partial u}{\partial x} \tag{2}$$

$$\Delta u = k_{NN}\frac{\partial u}{\partial x} + k_{NM}\frac{\partial^2 w}{\partial x^2} \tag{3}$$

where, k_{MM}, k_{NN}, k_{MN} and k_{NM} are the flexibility constants. Also, in case of free transverse vibrations, no longitudinal displacement is assumed and the flexibility constants k_{NN}, k_{MN} and k_{NM} are considered to be small [36]. Hence, only the flexibility related to the bending moment k_{MM} is considered.

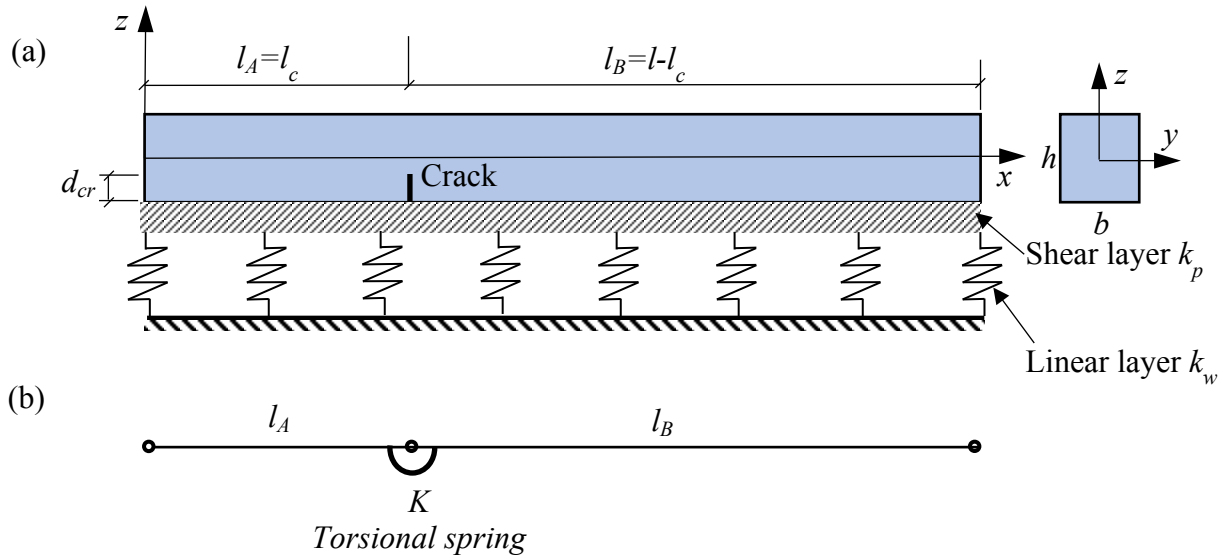

Fig. 1. (a): Cracked nanobeam on a Winkler-Pasternak elastic foundation, (b): crack is modelled as a torsional spring.

The edge crack causes a discontinuity in the bending slope and the continuity condition for the Euler–Bernoulli beam in the cracked section $x = l_c$ is,

$$\Delta\theta = \frac{k_{MM}\partial^2 W(x)}{l \quad \partial x^2}\Big|_{x=l_c} = K\frac{\partial^2 W(x)}{\partial x^2}\Big|_{x=l_c} \tag{4}$$

where $K = \frac{k_{MM}}{l}$.

Also, the stiffness of the rotational spring may be related to the crack depth by the following relation [48]

$$K_s = \frac{EI}{l}\frac{1}{k^*} \tag{5}$$

where

$$k^* = \frac{h}{l}C(d_{cr}/h) \tag{6}$$

in which, according to [49]:

$$C\left(d_{cr}/h\right) = \frac{\left(d_{cr}/h\right)[2 - (d_{cr}/h)]}{0.9[\left(d_{cr}/h\right) - 1]^2} \quad (7)$$

2.2 Nonlocal Elasticity Theory

Nonlocal elasticity theory [5] incorporates the size effects by adding a scale parameter to the classical continuum elasticity theory. For a nanobeam with length l and modulus of elasticity E, the stress at a general point x is given by

$$\sigma_{xx} = \int_0^l E\alpha_0(x,x',e_0a)\varepsilon'_{xx}(x')dx' \quad (8)$$

where ε'_{xx} is the normal strain at a neighbouring point x'. The coefficient α_0 is the principal attenuation kernel function, that imports the nonlocal effects to the constitutive equations. The parameter e_0a is the nonlocal coefficient, which represents the contribution of the nonlocal stress field, where a is an internal characteristic length and e_0 is the nonlocal material constant. Although, to date, no agreement has been achieved on how to specify the material-dependent length scale parameter experimentally [50], some studies have extracted the nonlocal parameter by molecular dynamics simulations in CNTs [51,52]. In this paper a parametric study is performed to analyse the effect of this parameter on the vibration behaviour of cracked nanobeams. Equation (5) denotes the weighted average of the contributions of the strain field at all points in the continuum over the stress field at a given point. The integral form of Eq. (8) is difficult to solve, but based on the linear differential operator that was proposed by Eringen [5], it is possible to transform the exponential nonlocal kernel functions to their equivalent differential form as follows

$$\left(1 - (e_0a)^2\nabla^2\right)\boldsymbol{\sigma} = \boldsymbol{C} : \boldsymbol{\varepsilon} \quad (9)$$

where $\nabla^2 = \frac{\partial^2}{\partial x^2} + \frac{\partial^2}{\partial y^2} + \frac{\partial^2}{\partial z^2}$ is the Laplacian operator.

2.3 Euler- Bernoulli Beam Theory Based on Nonlocal Elasticity

The displacement field (u_x,u_y,u_z) based on Euler-Bernoulli beam theory (EBT) at time t is given by

$$u_x(x,z,t) = u(x,t) - z\frac{\partial w(x,t)}{\partial x} \quad (10)$$

$$u_y(x,z,t) = 0 \quad (11)$$

$$u_z(x,z,t) = w(x,t) \tag{12}$$

where, u and w are the displacement components of the mid-surface in the axial (x) and transverse (z) directions, respectively. The non-zero normal strain of EBT is given by

$$\varepsilon_{xx} = \frac{\partial u_x}{\partial x} = \frac{\partial u}{\partial x} - z\frac{\partial^2 w}{\partial x^2} \tag{13}$$

In order to obtain the governing equations, Hamilton's principle is used

$$\delta\int_{t_1}^{t_2}(T - (U + V)dt = 0 \tag{14}$$

where, U, W and T denote the strain energy, the work done by the external forces and the kinetic energy, respectively.

The variation of the strain energy is defined as

$$\delta U = \int_V \sigma_{xx}\delta\epsilon_{xx}dV = \int_0^l \left(N_{xx}\frac{\partial\delta u}{\partial x} - M_{xx}\frac{\partial^2\delta w}{\partial x^2}\right)dx \tag{15}$$

where N_{xx} and M_{xx} denote the stress resultants corresponding to the axial forces and the bending moments respectively and are given by

$$N_{xx} = \int_A \sigma_{xx}dA \tag{16}$$

$$M_{xx} = \int_A z\sigma_{xx}dA \tag{17}$$

The variation of the kinetic energy is

$$\delta T = \int_0^l \rho A(\dot{u}\delta\dot{u} + \dot{w}\delta\dot{w})dx \tag{18}$$

The variation of the virtual work of the distributed axial load (f) and the distributed transverse load (q) and the concentrated axial end force P are defined as

$$\delta W = \int_0^l \left(f\delta u + q\delta w + P\frac{\partial w\partial\delta w}{\partial x\ \partial x}\right)dx \tag{19}$$

By substituting Eqs. (15), (18) and (19) into Eq. (14) and performing integration by parts the following weak form is derived

$$\int_{t_1}^{t_2}\int_0^l \left[\left(\frac{\partial N_{xx}}{\partial x} - f - \rho A\ddot{u}\right)\delta u + \left(\frac{\partial^2 M_{xx}}{\partial x^2} - q - \rho A\ddot{w} - P\frac{\partial^2 w}{\partial x^2}\right)\delta w\right]dxdt = 0 \tag{20}$$

By setting the coefficients of δu and δw to zero, the equation of motion for an Euler- Bernoulli beam is obtained as

$$\frac{\partial N_{xx}}{\partial x} - f = \rho A\ddot{u}, \tag{21}$$

$$\frac{\partial^2 M_{xx}}{\partial x^2} - q - P\frac{\partial^2 w}{\partial x^2} = \rho A\ddot{w} \tag{22}$$

Substituting Eq. (13) into Eq. (9), for a 1-dimensional element the following is derived

$$\sigma_{xx} - (ea_0)^2\frac{\partial^2\sigma_{xx}}{\partial x^2} = E\left(\frac{\partial u}{\partial x} - z\frac{\partial^2 w}{\partial x^2}\right) \tag{23}$$

In view of Eqs. (21) and (22), the stress resultants can be written as

$$N_{xx} = (ea_0)^2\frac{\partial^2 N_{xx}}{\partial x^2} + EA\frac{\partial u}{\partial x} \tag{24}$$

$$M_{xx} = (ea_0)^2\frac{\partial^2 M_{xx}}{\partial x^2} - EI\frac{\partial^2 w}{\partial x^2} \tag{25}$$

By using Eqs. (21), (22), (24) and (25), the governing equations of motion for an Euler-Bernoulli beam with respect to the displacements, and including nonlocal elasticity theory, are obtained as

$$EA\frac{\partial^2 u}{\partial x^2} + \left(1 - (ea_0)^2\frac{\partial^2}{\partial x^2}\right)(\rho A\ddot{u} - f) = 0 \tag{26}$$

$$EI\frac{\partial^4 w}{\partial x^4} + \left(1 - (ea_0)^2\frac{\partial^2}{\partial x^2}\right)\left(\rho A\ddot{w} + q + P\frac{\partial^2 w}{\partial x^2}\right) = 0 \tag{27}$$

In this study, the thermal transverse free vibrations are investigated, and therefore only Eq. (27) will be analysed. Also, the effect of thermal loading is considered via the axial force P, where

$$P = EA\varepsilon_{mechanical} = -EA\varepsilon_{thermal} = -EA\alpha\Delta T \tag{28}$$

where α is the linear thermal expansion coefficient and ΔT is the temperature change.

Assuming $w(x,t) = W(x)e^{i\omega t}$ and $q = k_w w - k_p\frac{\partial^2 w}{\partial x^2}$ the residue is given by

$$\mathrm{R}=\left\{EI\frac{d^4W}{dx^4} + \left(1 - (ea_0)^2\frac{d^2}{dx^2}\right)\left(\rho A\omega^2 W + k_w W - k_p\frac{d^2W}{dx^2} - EA\alpha\Delta T\frac{d^2W}{dx^2}\right)\right\} \tag{29}$$

Here, ω is the frequency, k_w is the linear stiffness related to the Winkler foundation, k_p is the shear stiffness corresponding to the Pasternak foundation and A is the cross section area,

2.4 Finite Element Formulation

Fig.2 shows a three-node beam element, where in this study the third node is assumed to be located at the crack and in the middle of the element ($l_a = l_b = l/2$). This finite beam element has seven degrees-of freedom including three transverse and four rotational displacements that are defined at the neutral axis.

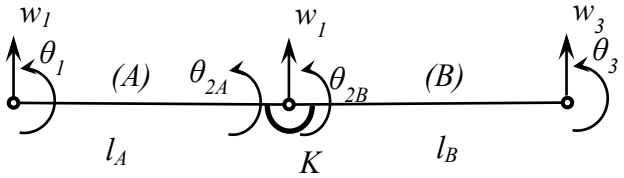

Fig. 2. Beam element with three nodes and seven degrees of freedom.

By minimizing Eq. (29) over a given element, one obtains

$$\int_0^l R\varphi dx = 0 \tag{30}$$

where φ is the weighting function in the Galerkin finite element method. This weighting function is also employed as the shape function. By substituting Eq. (29) into Eq. (30) and after performing partial integration, the weak form is derived as

$$\int_0^l \left[EI\frac{\partial^2 W \partial^2 \varphi}{\partial x^2\,\partial x^2} - \rho A\omega^2\left(W\varphi + (ea_0)^2\frac{\partial W\partial\varphi}{\partial x\,\partial x}\right) + k_p\frac{\partial W\partial\varphi}{\partial x\,\partial x} + (ea_0)^2 k_p\frac{\partial^2 W\partial^2\varphi}{\partial x^2\,\partial x^2} + k_w W\varphi + (ea_0)^2 k_w\frac{\partial W\partial\varphi}{\partial x\,\partial x}\right]dx$$

$$-(ea_0)^2\rho A\omega^2\frac{\partial W\partial\varphi}{\partial x\,\partial x}\Big|_0^l + (ea_0)^2(k_p - EA\alpha\Delta T)\frac{\partial W}{\partial x}\varphi\Big|_0^l - (ea_0)^2\left(k_p\frac{\partial W}{\partial x} - EA\alpha\Delta T\right)\frac{\partial^2 W\partial\varphi}{\partial x^2\,\partial x}\Big|_0^l + EI$$

$$\frac{\partial^3 W}{\partial x^3}\varphi\Big|_0^l - EI\frac{\partial^2 W\partial\varphi}{\partial x^2\,\partial x}\Big|_0^l - (k_p - EA\alpha\Delta T)\frac{\partial W}{\partial x}\varphi\Big|_0^l = 0 \tag{31}$$

The domain of the Euler-Bernoulli beam is discretized into a number of elements. The weak form is used for each of the discrete elements of length l_e with domain $\mho^e = (x_e, x_{e+1})$.

The general form of Eq. (31) for all nodes corresponding to a single element is obtained as

$$\int_0^{l_e}\left[EI\frac{\partial^2\varphi\partial^2\varphi}{\partial x^2\,\partial x^2} - \rho A\omega^2\left(\varphi\varphi + (ea_0)^2\frac{\partial\varphi\partial\varphi}{\partial x\,\partial x}\right) + (k_p - EA\alpha\Delta T)\frac{\partial\varphi\partial\varphi}{\partial x\,\partial x} + (ea_0)^2(k_p - EA\alpha\Delta T)\frac{\partial^2\varphi\partial^2\varphi}{\partial x^2\,\partial x^2} + k_w\varphi\varphi + (ea_0)^2 k_w\right.$$
$$= 0 \tag{32}$$

In this study, the finite element model is developed based on Hermit Interpolation functions for each of the left (A) and right (B) sections of the beam element. Each section is defined by four degrees of freedom and hence needs four interpolating polynomials defined as

$$\varphi = \begin{matrix}\left[\frac{1}{4}\left(1-\frac{x}{l_e}\right)^2(2+x/l_e)\right. \\ \frac{1}{8}l\left(1-\frac{x}{l_e}\right)^2(1+x/l_e) \\ \frac{-1}{8}l\left(1+\frac{x}{l_e}\right)^2(1-x/l_e) \\ \left.\frac{1}{4}\left(1+\frac{x}{l_e}\right)^2(2-x/l_e)\right]\end{matrix} \tag{33}$$

The dynamic equation for a beam is given by

$$\overline{\boldsymbol{M}}\ddot{\boldsymbol{U}} - (\overline{\boldsymbol{K}} + \overline{\boldsymbol{K}}_{\boldsymbol{T}})\boldsymbol{U} = \boldsymbol{0} \tag{34}$$

where, $\overline{\boldsymbol{K}}$, $\overline{\boldsymbol{M}}$ and $\overline{\boldsymbol{K}}_{\boldsymbol{T}}$ are the global stiffness, mass and thermal geometric stiffness matrices, respectively. $\boldsymbol{U}$ denotes the global displacement vector. For free vibration analysis, the following eigenvalue equation is deduced from Eq. (34)

$$(\overline{\boldsymbol{K}} + \overline{\boldsymbol{K}}_{\boldsymbol{T}} - \omega^2\overline{\boldsymbol{M}})\boldsymbol{U} = \boldsymbol{0} \tag{35}$$

where,

$$[\overline{\boldsymbol{K}}] = EI\boldsymbol{K} + k_w\boldsymbol{X}_1 + (ea_0)^2k_w\boldsymbol{X}_2 + k_p\boldsymbol{X}_2 + (ea_0)^2k_p\boldsymbol{K}, \tag{36}$$

$$[\overline{\boldsymbol{M}}] = \rho A\boldsymbol{X}_1 + (ea_0)^2\rho A\boldsymbol{X}_2. \tag{37}$$

$$[\overline{\boldsymbol{K}}_T] = -EA\alpha\Delta T(\boldsymbol{X}_2 + (ea_0)^2\boldsymbol{K}), \tag{38}$$

where the 4×4 element matrices of $\boldsymbol{K}$, $\boldsymbol{X}_1$and $\boldsymbol{X}_2$ for each uncracked beam element, and also the sections of the cracked beam element, are given in the Appendix. These elemental matrices are assembled in the standard way to build the global stiffness, mass and geometric matrices. Finally, these eigenvalue problems could be solved readily.

In order to study finite element of a cracked beam, the crack is modelled as a torsional spring connecting two elements with corresponding lengths of l_A and l_B, each side of a single edge crack, as shown in Fig. 2. The assembled stiffness matrix for this kind of element has the form [53]:

$$[K] = \begin{array}{c} \\ w_1 \\ \theta_1 \\ \theta_{2A} \\ w_2 \\ \theta_{2B} \\ \theta_3 \\ w_3 \end{array} \begin{array}{c} \begin{array}{ccccccc} \quad & \quad & \quad & \quad & \quad & \quad & \quad \end{array} \\ \begin{bmatrix} k_{11}^A & k_{12}^A & k_{13}^A & k_{14}^A & 0 & 0 & 0 \\ k_{21}^A & k_{22}^A & k_{23}^A & k_{24}^A & 0 & 0 & 0 \\ k_{31}^A & k_{32}^A & k_{33}^A + K & k_{34}^A & -K & 0 & 0 \\ k_{41}^A & k_{42}^A & k_{43}^A & k_{44}^A + k_{11}^B & k_{12}^B & k_{13}^B & k_{14}^B \\ 0 & 0 & -K & k_{21}^B & k_{22}^B + K & k_{23}^B & k_{24}^B \\ 0 & 0 & 0 & k_{31}^B & k_{32}^B & k_{33}^B & k_{34}^B \\ 0 & 0 & 0 & k_{41}^B & k_{42}^B & k_{43}^B & k_{44}^B \end{bmatrix} \end{array} \tag{39}$$

where k_{ij}^A and k_{ij}^B $(i,j = 1{:}4)$, refer to elements of the stiffness matrices for the portions of the beam A and the beam B, which are coupled by a torsional spring with stiffness K.

3. Numerical results

In the following subsections, first validity of the present model is investigated with the available studies in the literature, then a parametric examination is performed to analyse the thermal vibration behaviour of a cracked nanobeam on a Winkler- Pasternak elastic foundation with

different crack depth, crack location, temperature parameter, foundation stiffness, nonlocal parameter and boundary conditions. The following nondimensional parameters are employed

$$\hat{\omega}^4 = \omega^2 l^4 \frac{\rho A}{EI}, \quad K_w = \frac{k_w l^4}{EI}, \quad K_p = \frac{k_p l^2}{EI}, \quad P_{temp} = \frac{EA\alpha\Delta T l^2}{EI} \tag{40}$$

where $\hat{\omega}$, K_w, K_p and P_{temp} are the nondimensional frequency, Winkler stiffness, Pasternak stiffness and temperature parameter, respectively.
Also, the frequency ratio is defined as

$$\Omega = \frac{Natural\ frequency\ of\ a\ cracked\ beam}{Natural\ frequncy\ of\ an\ intact\ beam} \tag{41}$$

3.1 Validation

In order to present a thorough verification procedure, the influences of the crack severity and location, nonlocal parameter, foundation stiffness and temperature gradient are calculated individually and compared with the corresponding benchmark studies in the literature. Initially, the existence of the crack is neglected and the results are obtained for an intact beam on an elastic foundation (Tables 1 and 2). Then, the natural frequencies for a cracked nonlocal beam without an elastic foundation are calculated and compared (Tables 4 and 5). Finally, in Table 6, in order to analyse the thermal effects, the influences of both the foundation and the crack are ignored and different frequencies are obtained for various temperature parameters.
The first five nondimensional frequencies $\hat{\omega}$ for pinned-pinned beams with different Winkler-Pasternak foundation parameters are compared with those from Demir and Civalek [16], Togun and Bagdatli [54], Mustafa and Zhong [12] and Yokoyama [55] in Table 1. Based on these results, it is seen that good agreement is achieved between the five studies.

Table 1. Nondimensional frequencies $\hat{\omega}$ for pinned-pinned boundary conditions.

Mode number	Nondimensional Frequencies $\hat{\omega}$								
	$K_w = 25, K_p = 25$					$K_w = 36, K_p = 36$			
	Present	Demir and Civalek [16]	Togun and Bagdatli [54]	Mustafa and Zhong [12]	Yokoyama [55]	Present	Demir and Civalek [16]	Togun and Bagdatli [54]	Mustafa and Zhong [12]
1	19.2016	19.2133	19.2133	19.2178	19.21	22.1186	22.1069	22.1069	22.1112
2	50.6688	50.7004	50.7002	50.7804	50.71	54.8989	54.9162	54.916	55.1873
3	100.6473	100.6794	100.677	-	-	105.4515	105.4724	105.47	-
4	169.9863	170.0439	170.028	-	-	175.0559	175.1085	175.093	-
5	258.9208	259.0480	258.987	-	-	264.1314	264.2556	264.196	-

Also, a comparison is carried out between the results of the present model and those of Togun and Bagdatli [46]. Here, the first four nondimensional natural frequencies $\hat{\omega}$ for a nonlocal beam embedded in a Winkler-Pasternak medium are evaluated and compared for pinned-pinned and fixed-fixed boundary conditions in Tables 2 and 3, respectively.

Table 2. First four nondimensional frequencies $\hat{\omega}$ for different nonlocal parameters $e_0 a/l$ with pinned-pinned boundary conditions.

$e_0 a/l$	Nondimensional Frequencies $\hat{\omega}$			
	$K_w = 10, K_p = 5$			
	ω_1	ω_2	ω_3	ω_4

	Present	Togun and Bagdatli [54]	Present	Togun and Bagdatli [54]	Present	Togun and Bagdatli [54]	Present	Togun and Bagdatli [54]
0.0	12.5146	12.5203	42.0126	42.0231	91.3260	91.3470	160.383	160.4250
0.1	12.1636	12.1658	36.3884	36.3978	68.0447	68.0635	102.2853	102.3140
0.2	11.3636	11.3660	28.4815	28.4900	46.7512	46.7661	64.8468	64.8678
0.3	10.5297	10.5325	23.4372	23.4457	36.4738	36.4878	49.3651	49.3844
0.4	9.8513	9.85475	20.4945	20.5039	31.1748	31.1898	41.8001	41.8205
0.5	9.3468	9.35098	18.7183	18.7291	28.1633	28.1803	37.6017	37.6247

Table 3. First four nondimensional frequencies $\hat{\omega}$ for different nonlocal parameters e_0a/l with fixed-fixed boundary conditions.

e_0a/l	Nondimensional Frequencies $\hat{\omega}$							
	$K_w = 10, K_p = 5$							
	ω_1		ω_2		ω_3		ω_4	
	Present	Togun and Bagdatli [54]	Present	Togun and Bagdatli [54]	Present	Togun and Bagdatli [54]	Present	Togun and Bagdatli [54]
0.0	23.9126	23.9143	63.5714	63.5888	122.9359	122.972	201.9627	202.019
0.1	23.0764	23.0822	53.8200	53.8346	89.2658	89.2907	125.6068	125.6420
0.2	21.2793	21.2855	41.0222	41.035	60.6079	60.6274	79.1712	79.1969
0.3	19.5227	19.5297	33.3379	33.3506	47.3692	47.3877	60.3096	60.3333
0.4	18.1785	18.1866	29.0045	29.0183	40.6586	40.6783	51.1188	51.1438
0.5	17.2264	17.2362	26.4374	26.4531	36.8696	36.8920	46.0198	46.0480

For a pinned-pinned boundary condition, the first four nondimensional natural frequencies of a cracked nonlocal beam are given in Table 4 and compared with those of Torabi and Dastgerdi [26] and Loya et al. [36] which are based on Timoshenko beam theory (TBT) and Euler-Bernoulli (EBT) beam theory, respectively. For further validation, the nondimensional frequencies $\hat{\omega}$ of the present model are compared with those of Loya et al. [36] for fixed-fixed boundary conditions in Table 5. In this comparison first four vibration modes are again analysed.

Table 4. Comparison of first four nondimensional frequencies $\hat{\omega}$ for a pinned-pinned beam with different nonlocal parameters e_0a/l and crack severities K.

			$e_0a/l = 0$			$e_0a/l = 0.2$		
l_c	K	Mode number	TBT Torabi [26]	EBT Loya [36]	EBT Present	TBT Torabi [26]	EBT Loya [36]	EBT Present
0.5	0	1	3.1252	3.1416	3.1409	2.8795	2.8908	2.8907
		2	6.1583	6.2832	6.2818	4.9225	4.9581	4.9578
		3	9.0328	9.4248	9.4228	6.4222	6.4520	6.4517
		4	11.7170	12.5664	12.5638	7.6262	7.6407	7.6403
	0.065	1	2.9379	3.0469	3.0466	2.7290	2.8031	2.8030
		2	6.1583	6.2832	6.2818	4.9225	4.9581	4.9578
		3	8.5536	9.1669	9.1652	6.1820	6.2604	6.2601
		4	11.7170	12.5664	12.5638	7.6262	7.6407	7.6403
	0.35	1	2.3533	2.7496	2.7489	2.2387	2.5233	2.5232
		2	6.1583	6.2832	6.2819	4.9225	4.9581	4.9578
		3	7.3535	8.6129	8.6114	5.5861	5.7891	5.7889

		4	11.7170	12.5664	12.5638	7.6262	7.6407	7.6403
	2	1	1.3055	2.0960	2.0958	1.2842	1.9098	1.9098
		2	6.1583	6.2832	6.2818	4.9225	4.9581	4.9578
		3	6.3928	8.0730	8.0715	5.2078	5.3416	5.3413
		4	11.7170	12.5664	12.5638	7.6262	7.6407	7.6403
0.25	0	1	3.1252	3.1416	3.1409	2.8795	2.8908	2.8908
		2	6.1583	6.2832	6.2818	4.9225	4.9580	4.9580
		3	9.0328	9.4248	9.4228	6.4222	6.4520	6.4519
		4	11.7170	12.5664	12.5638	7.6262	7.6407	7.6405
	0.065	1	3.024	3.0921	3.0925	2.7985	2.8447	2.8446
		2	5.8101	6.1028	6.1019	4.7165	4.8101	4.8100
		3	8.8166	9.3021	9.3005	6.3146	6.3638	6.3637
		4	11.717	12.5664	12.5642	7.6262	7.6407	7.6405
	0.35	1	2.596	2.9071	2.9064	2.4461	2.6645	2.6645
		2	4.9441	5.6491	5.6484	4.1829	4.4169	4.4168
		3	8.4026	9.0767	9.0752	6.1179	6.1924	6.1923
		4	11.717	12.5664	12.5642	7.6262	7.6407	7.6405
	2	1	1.5023	2.3493	2.3465	1.4703	2.1134	2.1134
		2	4.3015	5.1047	5.1042	3.7556	3.9906	3.9906
		3	8.1377	8.9008	8.8993	5.9940	6.0692	6.0691
		4	11.717	12.5664	12.5642	7.6262	7.6407	7.6405

Table 5. Comparison of first four nondimensional frequencies $\hat{\omega}$ for a fixed-fixed beam with different nonlocal parameters e_0a/l and crack severities K.

			$e_0a/l=0$		$e_0a/l=0.2$	
l_c	K	Mode number	EBT Loya [36]	EBT Present	EBT Loya [36]	EBT Present
0.5	0	1	4.7300	4.7291	4.2766	4.2764
		2	7.8532	7.8516	6.0352	6.035
		3	10.9956	10.9934	7.3840	7.3837
		4	14.1372	14.1343	8.4624	8.4621
	0.065	1	4.6285	4.6277	4.1736	4.1735
		2	7.8532	7.8516	6.0352	6.035
		3	10.6976	10.6957	7.1421	7.1419
		4	14.1372	14.1343	8.4624	8.4621
	0.35	1	4.3566	4.356	3.8855	3.8854
		2	7.8532	7.8516	6.0352	6.035
		3	10.1028	10.101	6.6089	6.6087
		4	14.1372	14.1343	8.4624	8.4621
	2	1	3.9702	3.9696	3.4764	3.4763
		2	7.8532	7.8517	6.0352	6.035
		3	9.5833	9.5815	6.2045	6.2043
		4	14.1372	14.1343	8.4624	8.4621
0.25	0	1	4.7300	4.7312	4.2766	4.2765
		2	7.8532	7.8521	6.0352	6.0351
		3	10.9956	10.9949	7.3840	7.3839
		4	14.1372	14.1357	8.4490	8.4622
	0.065	1	4.7273	4.7261	4.2752	4.2751
		2	7.6991	7.6989	5.9062	5.9061
		3	10.7787	10.7776	7.1962	7.1961
		4	14.0911	14.0894	8.3902	8.3901
	0.35	1	4.7194	4.7145	4.2705	4.2704
		2	7.3175	7.3175	5.5040	5.5039

		3	10.4067	10.4048	6.8797	6.8796
		4	14.0159	14.0146	8.2780	8.2778
	2	1	4.7068	4.7038	4.2595	4.2594
		2	6.8770	6.8766	5.0234	5.0233
		3	10.1452	10.1441	6.7231	6.723
		4	13.9634	13.9618	8.2163	8.2161

For further validation, the nondimensional thermal frequencies for different temperature parameters P_{temp}, nonlocal coefficients $e_0 a/l$ and boundary conditions are given in Table 6 and compared with those given by Demir and Civalek [16].

Table 6. Nondimensional natural frequencies $\hat{\omega}$ for different nonlocal parameters $e_0 a/l$ and thermal effects P_{temp}.

P_{temp}	$e_0 a/l$					
	0		0.1		0.2	
	Present	Demir& Civalek [16]	Present	Demir& Civalek [16]	Present	Demir& Civalek [16]
	Pinned-pinned					
0	3.1415	3.1416	3.0680	3.0685	2.8903	2.8908
1	3.0563	3.0588	2.9787	2.9793	2.7823	2.7828
2	2.968	2.9687	2.8806	2.8813	2.6599	2.6605
3	2.8694	2.8695	2.7714	2.7721	2.5179	2.5185
	Fixed-fixed					
0	4.7292	4.7300	4.5936	4.5945	4.2759	4.2766
1	4.6993	4.7007	4.5532	4.5541	4.2047	4.2054
2	4.6696	4.6707	4.5117	4.5125	4.1296	4.1304
3	4.6397	4.6402	4.4689	4.4697	4.0503	4.0510
	Pinned-pinned					
0	3.1415	3.1416	3.068	3.0685	2.8903	2.8908
-1	3.218	3.2183	3.1501	3.1506	2.9875	2.9880
-2	3.2894	3.2899	3.2262	3.2267	3.0759	3.0764
-3	3.3562	3.3571	3.2973	3.2977	3.1574	3.1579
	Fixed-fixed					
0	4.7292	4.7300	4.5936	4.5945	4.2759	4.2766
-1	4.7582	4.7588	4.633	4.6338	4.3436	4.3444
-2	4.7861	4.7871	4.6713	4.6721	4.4084	4.4092
-3	4.814	4.8148	4.7087	4.7095	4.4703	4.4712

This concludes the thorough validation procedure for the present model. Good agreement is achieved between the results of this study and the benchmark investigations from the literature.

3.2 Thermal vibration of a cracked nanobeam on an elastic foundation

In this section, a parametric study is performed to analyse the thermal vibration behaviour of a cracked nanobeam $(l = 100h,\ h = 1\text{nm})$ on an elastic foundation with various crack depth, crack location, temperature parameter, foundation stiffness, nonlocal parameter and boundary conditions.

Fig.3, shows the variation of the nondimensional frequencies of the cracked nanobeam with the temperature parameter P_{temp} for various crack severities K and boundary conditions. The frequencies decrease as the crack severity increases, which is related to the stiffness reduction in the cracked beams. In this study, the thermal expansion coefficient is assumed to be positive, which means that as temperature reduces, the beam stretches and this results in higher stiffness, which causes higher frequencies. Moreover, the crack severity has a unique influence on the frequencies for each boundary condition. As an illustration, the frequencies for the fixed-fixed boundary condition have the least dependence on the variation of the crack severity, while the frequencies related to the pinned-pinned boundary condition have the highest dependence on the crack severity change, among the three boundary conditions that are investigated in this study.

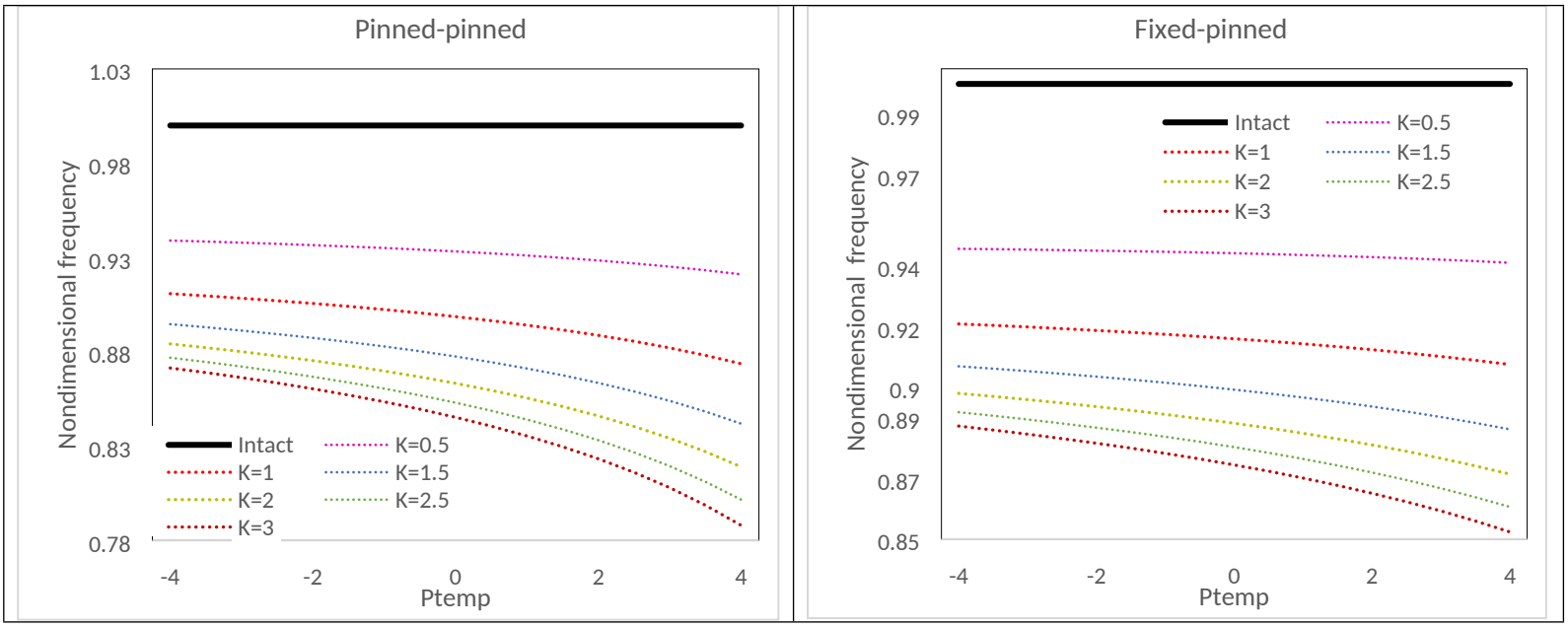

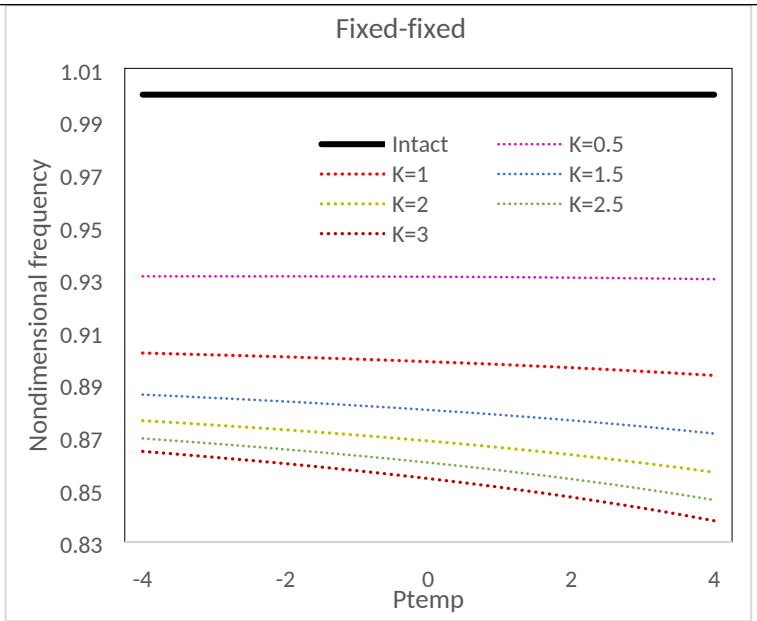

Fig.3. Variation of the nondimensional frequencies with the temperature parameter P_{temp} for different crack severities K and boundary conditions ($e_0 a/l = 0.2, K_w = 10, K_P = 5, l_c = 0.5$).

Variations of the first three natural frequency ratios Ω of the cracked nanobeam with respect to the crack position for two temperature parameters P_{temp} and different boundary conditions are plotted in Fig. 4. In all four cases, the first mode of the vibration is the case where the thermal effects create the most difference in the frequency ratio and for the higher modes the influence of the temperature parameter reduces and the two temperatures ($P_{temp} = 0, P_{temp} = 4$) have similar trends. Furthermore, considering the fixed-fixed beam, the temperature parameter (P_{temp}) has the minimum effect on the frequency ratio, while for a pinned-pinned beam, the effect of the temperature parameter on the frequency ratio is maximum among the boundary conditions considered. Another interesting point is that, because of the symmetry of the model, the second natural frequency corresponding to the mid-span cracked beam is independent of the crack severity; these results were expected since the second derivative of the transverse displacement is zero at the midpoint of the beam.

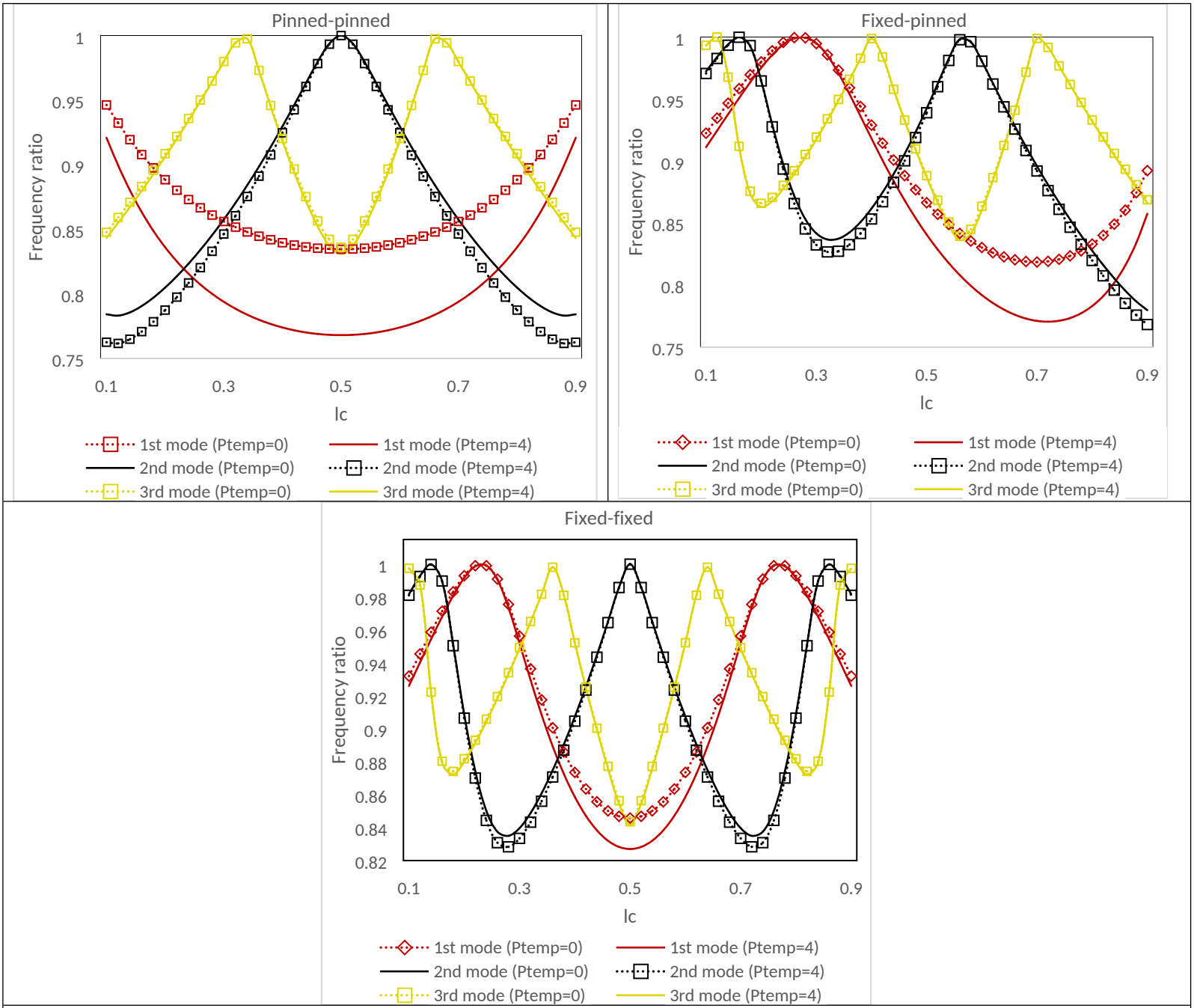

Fig. 4. Variations of the first three frequency ratios Ω of cracked nanobeam with respect to crack position for two temperature parameters P_{temp} and different boundary conditions ($e_0a/l = 0.2, K_w = 10, K_P = 5$).

Fig.5 shows the variation of the nondimensional frequency $\hat{\omega}$ with the temperature parameter P_{temp} and crack severity K for local $e_0a/l = 0$ and nonlocal $e_0a/l = 0.2$, considering different boundary conditions and foundation stiffness. For a nanobeam without an elastic foundation, the variation of the nondimensional frequency with respect to the temperature parameter is nonlinear, while for a nanobeam resting on an elastic foundation this variation becomes linear. Also, the nonlocal effect is more significant for a nanobeam embedded in an elastic foundation. This is

because the nonlocal elasticity effect is also considered for elastic foundation in the formulations. Moreover, in this example, different ranges are assumed for the temperature parameters P_{temp}, because, for pinned-pinned boundary condition, the beam loses its static stability for temperature parameters greater than $P_{temp} = 2$.

$K_w = 0, K_p = 0$	$K_w = 100, K_p = 50$
Pinned-pinned	
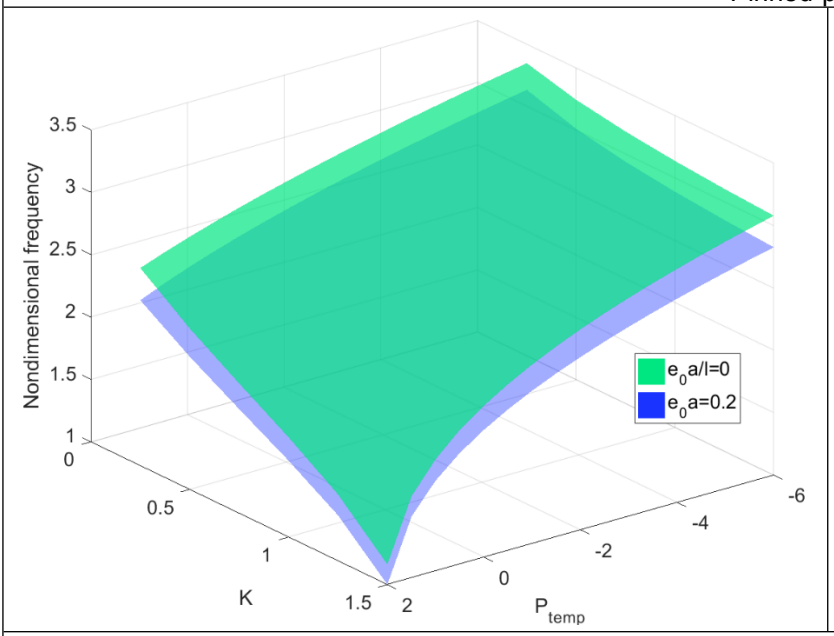	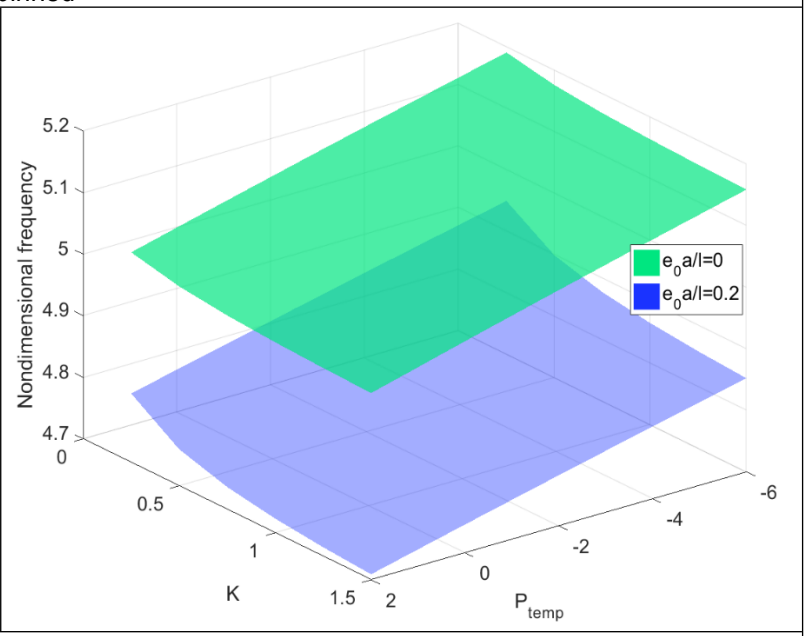
Fixed-pinned	
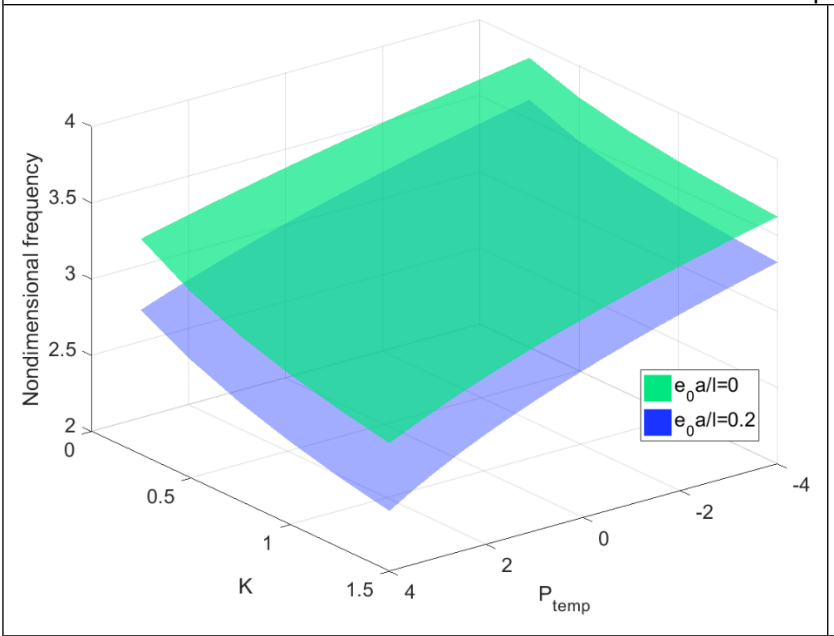	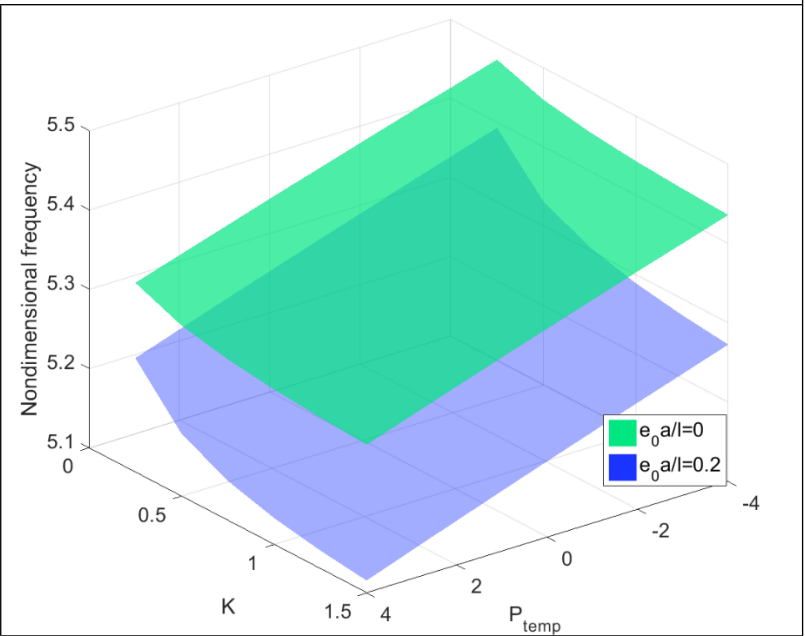
Fixed-fixed	

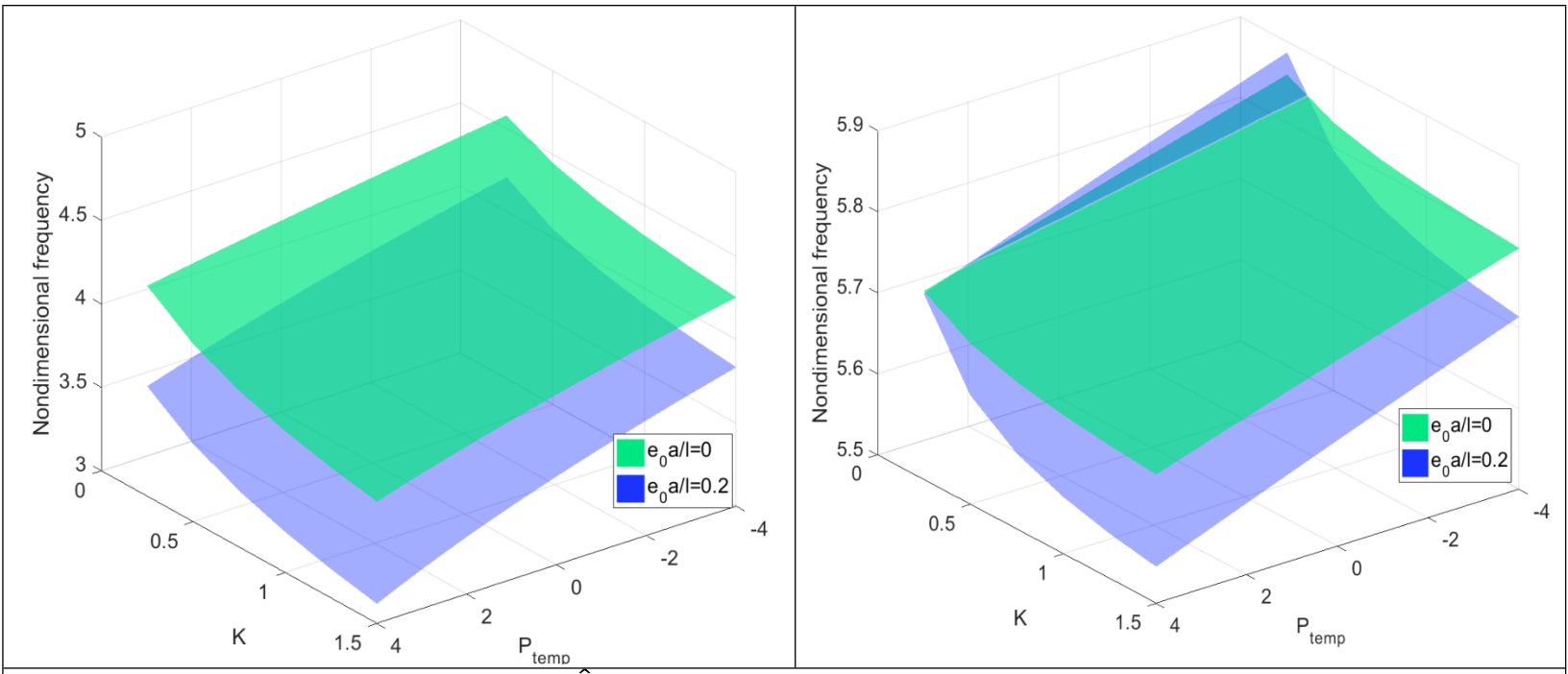

Fig.5. Variation of the nondimensional frequency $\hat{\omega}$ with temperature parameter P_{temp} and crack severity K for local $e_0a/l = 0$ and nonlocal $e_0a/l = 0.2$ cases, considering different boundary conditions and foundation stiffness ($l_c = 0.5$).

The changes of the nondimensional fundamental frequency $\hat{\omega}$ for pinned-pinned, fixed-pinned and fixed-fixed beam with various crack severities K, foundation stiffnesses (K_w, K_P), temperature parameters P_{temp} and nonlocal parameters e_0a/l are given in Table 7 for a crack located at $l_c = 0.5$ and in Table 8 for a crack located at $l_c = 0.25$.

Table 7. Nondimensional natural frequency $\hat{\omega}$ of pinned-pinned, fixed-pinned and fixed-fixed boundary conditions for various crack severities K, elastic foundations (K_w, K_P), nonlocal parameters e_0a/l and temperature parameters P_{temp} $(l_c = 0.5)$.

Pinned-pinned							
K	(K_w, K_P)	e_0a/l=0			e_0a/l=0.2		
		P_{temp}			P_{temp}		
		-1	0	1	-2	0	2
Intact	(0,0)	3.1797	3.1409	3.1002	2.9405	2.8907	2.8382
	(10,5)	3.2553	3.2179	3.1804	3.0342	2.9891	2.9418
1	(0,0)	2.4776	2.3825	2.2753	2.2672	2.1778	2.0757
	(10,5)	2.6271	2.5490	2.4631	2.4566	2.3875	2.3118
2	(0,0)	2.2334	2.0958	1.9231	2.0376	1.9098	1.7494
	(10,5)	2.4307	2.3248	2.2043	2.2845	2.1971	2.0978
3	(0,0)	2.1007	1.9260	1.6806	1.9131	1.7528	1.5300
	(10,5)	2.3302	2.2062	2.0610	2.1992	2.0997	1.9835
Fixed-pinned							
K	(K_w, K_P)	e_0a/l=0			e_0a/l=0.2		

		P_{temp}			P_{temp}		
		-2	0	2	-2	0	2
Intact	(0,0)	3.9490	3.9256	3.9019	3.6090	3.5700	3.5296
	(10,5)	3.9895	3.9664	3.9430	3.6611	3.6237	3.5851
1	(0,0)	3.4304	3.3892	3.3462	3.0984	3.0505	3.0003
	(10,5)	3.4908	3.4516	3.4116	3.1792	3.1350	3.0888
2	(0,0)	3.2994	3.2513	3.2006	2.9691	2.9145	2.8565
	(10,5)	3.3668	3.3217	3.2743	3.0604	3.0106	2.9582
3	(0,0)	3.2392	3.1872	3.1321	2.9103	2.8518	2.7894
	(10,5)	3.3106	3.2617	3.2101	3.0068	2.9540	2.8981
Fixed-fixed							
K	(K_w, K_P)	e_0a/l=0			e_0a/l=0.2		
		P_{temp}			P_{temp}		
		-2	0	2	-2	0	2
Intact	(0,0)	4.7434	4.7291	4.7145	4.3107	4.2764	4.2413
	(10,5)	4.7669	4.7525	4.7380	4.3416	4.3080	4.2737
1	(0,0)	4.1357	4.1073	4.0779	3.6595	3.6202	3.5795
	(10,5)	4.1707	4.1428	4.1143	3.7095	3.6718	3.6328
2	(0,0)	4.0030	3.9696	3.9350	3.5206	3.4763	3.4302
	(10,5)	4.0414	4.0088	3.9754	3.5765	3.5343	3.4905
3	(0,0)	3.9444	3.9085	3.8713	3.4603	3.4134	3.3644
	(10,5)	3.9844	3.9498	3.9137	3.5191	3.4746	3.4282

Table 8. Nondimensional natural frequency $\hat{\omega}$ of pinned-pinned, fixed-pinned and fixed-fixed boundary conditions for various crack severities K, elastic foundations (K_w, K_P), nonlocal parameters e_0a/l and temperature parameters P_{temp} $(l_c = 0.25)$.

Pinned-pinned							
K	(K_w, K_P)	e_0a/l=0			e_0a/l=0.2		
		P_{temp}			P_{temp}		
		-2	0	2	-2	0	2
Intact	(0,0)	3.1797	3.1409	3.1002	2.9405	2.8907	2.8382
	(10,5)	3.2553	3.2179	3.1804	3.0342	2.9891	2.9418
1	(0,0)	2.6950	2.6170	2.5300	2.4520	2.3753	2.2903
	(10,5)	2.8147	2.7465	2.6718	2.6063	2.5432	2.4749
2	(0,0)	2.4641	2.3493	2.2103	2.2221	2.1133	1.9841
	(10,5)	2.6174	2.5211	2.4130	2.4215	2.3393	2.2471
3	(0,0)	2.3264	2.1767	1.9844	2.0876	1.9501	1.7744
	(10,5)	2.5040	2.3873	2.2470	2.3204	2.2239	2.1124
Fixed-pinned							
K	(K_w, K_P)	e_0a/l=0			e_0a/l=0.2		
		P_{temp}			P_{temp}		
		-2	0	2	-2	0	2
Intact	(0,0)	3.9490	3.9256	3.9019	3.6090	3.5700	3.5296
	(10,5)	3.9895	3.9664	3.9430	3.6611	3.6237	3.5851
1	(0,0)	3.9462	3.9222	3.8977	3.5992	3.5596	3.5186
	(10,5)	3.9862	3.9631	3.9390	3.6516	3.6138	3.5746
2	(0,0)	3.9453	3.9213	3.8966	3.5964	3.5566	3.5154
	(10,5)	3.9857	3.9621	3.9378	3.6490	3.6109	3.5715
3	(0,0)	3.9450	3.9208	3.8960	3.5951	3.5552	3.5138
	(10,5)	3.9854	3.9618	3.9373	3.6478	3.6096	3.5701

Fixed-fixed							
K	(K_w, K_P)	e_0a/l=0			e_0a/l=0.2		
		P_{temp}			P_{temp}		
		-2	0	2	-2	0	2
Intact	(0,0)	4.7434	4.7291	4.7145	4.3107	4.2764	4.2413
	(10,5)	4.7669	4.7525	4.7380	4.3416	4.3080	4.2737
1	(0,0)	4.7249	4.7105	4.6958	4.2981	4.2640	4.2291
	(10,5)	4.7485	4.7343	4.7198	4.3292	4.2959	4.2617
2	(0,0)	4.7204	4.7059	4.6912	4.2935	4.2593	4.2243
	(10,5)	4.7441	4.7297	4.7151	4.3247	4.2913	4.2571
3	(0,0)	4.7183	4.7038	4.6891	4.2910	4.2569	4.2218
	(10,5)	4.7420	4.7276	4.7130	4.3223	4.2889	4.2547

4. Conclusions

In this paper the natural frequencies of cracked nanobeams on an elastic foundation, considering thermal effects, are investigated. To incorporate the size effect of the nanostructure, nonlocal elasticity theory was employed. The cracked section of the nanobeam was modelled using a rotational spring that gives a discontinuity in the slope, which is proportional to the crack severity. Three different boundary conditions were analysed: pinned-pinned, fixed-pinned and fixed-fixed. The finite element methodology used here, provides a simple formulation that enables the influence of important parameters (i.e. crack severity, crack location, thermal effects, nonlocal parameter and foundation stiffness) that appear in typical applications to be analysed accurately.

Appendix A

Beam element matrices are given by

$$K = \frac{1}{l^3}\begin{bmatrix} 12 & 6l & 6l & -12 \\ 6l & 4l^2 & 2l^2 & -6 \\ 6l & 2l^2 & 4l^2 & -6l \\ -12 & -6l & -6l & 12 \end{bmatrix} \tag{A.1}$$

$$X_1 = \frac{1}{420}\begin{bmatrix} 156l & 22l^2 & -13l^2 & 54l \\ 22l^2 & 4l^3 & -3l^3 & 13l^2 \\ -13l^2 & -3l^3 & 4l^3 & -22l^2 \\ 54l & 13l^2 & -22l^2 & 156l \end{bmatrix} \tag{A.2}$$

$$X_2 = \frac{1}{30l}\begin{bmatrix} 36 & 3l & 3l & -36 \\ 3l & 4l^2 & -l^2 & -3l \\ 3l & -l^2 & 4l^2 & -3l \\ -36 & -3l & -3l & 36 \end{bmatrix} \tag{A.3}$$

where l is the corresponding beam length on each side of the crack ($l_A = l_B = l$).

Data Availability

All of the results given in the paper are simulated based on the proposed finite element model. The paper contains full details of the developed finite element and the geometry and material properties for the examples. Hence, there is no raw data, and data in the figures and tables maybe be reproduced by coding the described model.

References

1. Lebaschi, A.H., Deng, X.H., Camp, C.L., Zong, J., Cong, G.T., Carballo, C.B., Album, Z. and Rodeo, S.A., 2018. Biomechanical, Histologic, and Molecular Evaluation of Tendon Healing in a New Murine Model of Rotator Cuff Repair. Arthroscopy: The Journal of Arthroscopic & Related Surgery, 34(4), pp.1173-1183.
2. Johnson, K.L., Gidley, M.J., Bacic, A. and Doblin, M.S., 2018. Cell wall biomechanics: a tractable challenge in manipulating plant cell walls 'fit for purpose'!. Current opinion in biotechnology, 49, pp.163-171.
3. Jandaghian, A.A. and Rahmani, O., 2017. Size-dependent free vibration analysis of functionally graded piezoelectric plate subjected to thermo-electro-mechanical loading. Journal of Intelligent Material Systems and Structures, 28(20), pp.3039-3053.
4. Şimşek, M., 2016. Nonlinear free vibration of a functionally graded nanobeam using nonlocal strain gradient theory and a novel Hamiltonian approach. International Journal of Engineering Science, 105, pp.12-27.
5. Eringen, A.C., 1983. On differential equations of nonlocal elasticity and solutions of screw dislocation and surface waves. Journal of applied physics, 54(9), pp.4703-4710.
6. Friswell, M.I., Adhikari, S. and Lei, Y., 2007. Vibration analysis of beams with non--local mediums using finite element method. International Journal for Numerical Methods in Engineering, 71(11), pp.1365-1386.
7. Barretta, R., Faghidian, S.A., Luciano, R., Medaglia, C.M. and Penna, R., 2018. Free vibrations of FG elastic Timoshenko nano-beams by strain gradient and stress-driven nonlocal models. Composites Part B: Engineering, 154, pp.20-32.
8. Phadikar, J.K. and Pradhan, S.C., 2010. Variational formulation and finite element analysis for nonlocal elastic nanobeams and nanoplates. Computational materials science, 49(3), pp.492-499.
9. Murmu, T. and Adhikari, S., 2010. Nonlocal transverse vibration of double-nanobeam-systems. Journal of Applied Physics, 108(8), p.083514.
10. Zhang, Y., Liew, K.M. and Hui, D., 2018. Characterizing nonlinear vibration behavior of bilayer graphene thin films. Composites Part B: Engineering, 145, pp.197-205.
11. Roque, C.M.C., Ferreira, A.J.M. and Reddy, J.N., 2011. Analysis of Timoshenko nanobeams with a nonlocal formulation and meshless method. International Journal of Engineering Science, 49(9), pp.976-984.
12. Mustapha, K.B. and Zhong, Z.W., 2010. Free transverse vibration of an axially loaded non--prismatic single-walled carbon nanotube embedded in a two-parameter elastic medium. Computational Materials Science, 50(2), pp.742-751.
13. Jalaei, M.H. and Arani, A.G., 2018. Size-dependent static and dynamic responses of embedded double-layered graphene sheets under longitudinal magnetic field with arbitrary boundary conditions. Composites Part B: Engineering, 142, pp.117-130.
14. Lei, Y., Adhikari, S. and Friswell, M.I., 2013. Vibration of nonlocal Kelvin–Voigt viscoelastic damped Timoshenko beams. International Journal of Engineering Science, 66, pp.1-13.
15. Civalek, Ö. and Demir, C., 2016. A simple mathematical model of microtubules surrounded by an elastic matrix by nonlocal finite element method. Applied Mathematics and Computation, 289, pp.335-352.
16. Demir, Ç. and Civalek, Ö., 2017. A new nonlocal FEM via Hermitian cubic shape functions for thermal vibration of nano beams surrounded by an elastic matrix. Composite Structures, 168, pp.872-884.

17. Ebrahimi, F. and Barati, M.R., 2017. Buckling analysis of nonlocal third-order shear deformable functionally graded piezoelectric nanobeams embedded in elastic medium. Journal of the Brazilian Society of Mechanical Sciences and Engineering, 39(3), pp.937-952.
18. Bahrami, A., 2017. A wave-based computational method for free vibration, wave power transmission and reflection in multi-cracked nanobeams. Composites Part B: Engineering, 120, pp.168-181.
19. Taati, E. and Sina, N., 2018. Multi-objective optimization of functionally graded materials, thickness and aspect ratio in micro-beams embedded in an elastic medium. Structural and Multidisciplinary Optimization, pp.1-21.
20. Aria, A.I. and Biglari, H., 2018. Computational vibration and buckling analysis of microtubule bundles based on nonlocal strain gradient theory. Applied Mathematics and Computation, 321, pp.313-332.
21. Zhang, K., Ge, M.H., Zhao, C., Deng, Z.C. and Xu, X.J., 2018. Free vibration of nonlocal Timoshenko beams made of functionally graded materials by Symplectic method. Composites Part B: Engineering.
22. Zhang, Y., Li, G. and Liew, K.M., 2018. Thermomechanical buckling characteristic of ultrathin films based on nonlocal elasticity theory. Composites Part B: Engineering, 153, pp.184-193.
23. Aria, A.I. and Friswell, M.I., 2018. A nonlocal finite element model for buckling and vibration of functionally graded nanobeams. Composites Part B: Engineering. https://doi.org/10.1016/j.compositesb.2018.11.071
24. Zhu, C.S., Fang, X.Q., Liu, J.X. and Li, H.Y., 2017. Surface energy effect on nonlinear free vibration behavior of orthotropic piezoelectric cylindrical nano-shells. European Journal of Mechanics-A/Solids, 66, pp.423-432.
25. Zhu, C.S., Fang, X.Q. and Liu, J.X., 2017. Surface energy effect on buckling behavior of the functionally graded nano-shell covered with piezoelectric nano-layers under torque. International Journal of Mechanical Sciences, 133, pp.662-673.
26. Torabi, K. and Dastgerdi, J.N., 2012. An analytical method for free vibration analysis of Timoshenko beam theory applied to cracked nanobeams using a nonlocal elasticity model. Thin Solid Films, 520(21), pp.6595-6602.
27. Areias, P., Rabczuk, T. and Msekh, M.A., 2016. Phase-field analysis of finite-strain plates and shells including element subdivision. Computer Methods in Applied Mechanics and Engineering, 312, pp.322-350.
28. Nguyen-Thanh, N., Valizadeh, N., Nguyen, M.N., Nguyen-Xuan, H., Zhuang, X., Areias, P., Zi, G., Bazilevs, Y., De Lorenzis, L. and Rabczuk, T., 2015. An extended isogeometric thin shell analysis based on Kirchhoff–Love theory. Computer Methods in Applied Mechanics and Engineering, 284, pp.265-291.
29. Amiri, F., Millán, D., Shen, Y., Rabczuk, T. and Arroyo, M., 2014. Phase-field modeling of fracture in linear thin shells. Theoretical and Applied Fracture Mechanics, 69, pp.102-109.
30. Areias, P. and Rabczuk, T., 2013. Finite strain fracture of plates and shells with configurational forces and edge rotations. International Journal for Numerical Methods in Engineering, 94(12), pp.1099-1122.
31. Chau-Dinh, T., Zi, G., Lee, P.S., Rabczuk, T. and Song, J.H., 2012. Phantom-node method for shell models with arbitrary cracks. Computers & Structures, 92, pp.242-256.
32. Rabczuk, T., Areias, P.M.A. and Belytschko, T., 2007. A meshfree thin shell method for non-linear dynamic fracture. International Journal for Numerical Methods in Engineering, 72(5), pp.524-548.
33. Rabczuk, T. and Areias, P., 2006. A meshfree thin shell for arbitrary evolving cracks based on an extrinsic basis.
34. Rabczuk, T., Gracie, R., Song, J.H. and Belytschko, T., 2010. Immersed particle method for fluid–structure interaction. International Journal for Numerical Methods in Engineering, 81(1), pp.48-71.
35. Luque, A., Aldazabal, J., Martínez-Esnaola, J.M. and Sevillano, J.G., 2006. Atomistic simulation of tensile strength and toughness of cracked Cu nanowires. Fatigue & Fracture of Engineering Materials & Structures, 29(8), pp.615-622.
36. Loya, J., López-Puente, J., Zaera, R. and Fernández-Sáez, J., 2009. Free transverse vibrations of cracked nanobeams using a nonlocal elasticity model. Journal of Applied Physics, 105(4), p.044309.
37. Hasheminejad, S.M., Gheshlaghi, B., Mirzaei, Y. and Abbasion, S., 2011. Free transverse vibrations of cracked nanobeams with surface effects. Thin Solid Films, 519(8), pp.2477-2482.
38. Hosseini-Hashemi, S., Fakher, M., Nazemnezhad, R. and Haghighi, M.H.S., 2014. Dynamic behavior of thin and thick cracked nanobeams incorporating surface effects. Composites Part B: Engineering, 61, pp.66-72.
39. Roostai, H. and Haghpanahi, M., 2014. Vibration of nanobeams of different boundary conditions with multiple cracks based on nonlocal elasticity theory. Applied Mathematical Modelling, 38(3), pp.1159-1169.
40. Karličić, D., Jovanović, D., Kozić, P. and Cajić, M., 2015. Thermal and magnetic effects on the vibration of a cracked nanobeam embedded in an elastic medium. Journal of Mechanics of Materials and Structures, 10(1), pp.43-62.

41. Beni, Y.T., Jafaria, A. and Razavi, H., 2014. Size effect on free transverse vibration of cracked nano-beams using couple stress theory. International Journal of Engineering-Transactions B: Applications, 28(2), pp.296-304.
42. Wang, K. and Wang, B., 2015. Timoshenko beam model for the vibration analysis of a cracked nanobeam with surface energy. Journal of Vibration and Control, 21(12), pp.2452-2464.
43. Khorshidi, M.A., Shaat, M., Abdelkefi, A. and Shariati, M., 2017. Nonlocal modeling and buckling features of cracked nanobeams with von Karman nonlinearity. Applied Physics A, 123(1), p.62.
44. Yang, X.D., Lim, C.W. and Liew, K.M., 2010. Vibration and stability of an axially moving beam on elastic medium. Advances in Structural Engineering, 13(2), pp.241-247.
45. Murmu, T. and Pradhan, S.C., 2009. Thermo-mechanical vibration of a single-walled carbon nanotube embedded in an elastic medium based on nonlocal elasticity theory. Computational Materials Science, 46(4), pp.854-859.
46. Amirian, B., Hosseini-Ara, R. and Moosavi, H., 2013. Thermal vibration analysis of carbon nanotubes embedded in two-parameter elastic medium based on nonlocal Timoshenko's beam theory. Archives of Mechanics, 64(6), pp.581-602.
47. Chang, T.P., 2012. Thermal–mechanical vibration and instability of a fluid-conveying single-walled carbon nanotube embedded in an elastic medium based on nonlocal elasticity theory. Applied Mathematical Modelling, 36(5), pp.1964-1973.
48. Caddemi, S. and Calio, I., 2009. Exact closed-form solution for the vibration modes of the Euler–Bernoulli beam with multiple open cracks. Journal of Sound and Vibration, 327(3-5), pp.473-489.
49. Caddemi, S. and Caliò, I., 2013. The exact explicit dynamic stiffness matrix of multi-cracked Euler–Bernoulli beam and applications to damaged frame structures. Journal of Sound and Vibration, 332(12), pp.3049-3063.
50. Khodabakhshi, P. and Reddy, J.N., 2015. A unified integro-differential nonlocal model. International Journal of Engineering Science, 95, pp.60-75.
51. Duan, W.H., Wang, C.M. and Zhang, Y.Y., 2007. Calibration of nonlocal scaling effect parameter for free vibration of carbon nanotubes by molecular dynamics. Journal of applied physics, 101(2), p.024305.
52. Arash, B. and Ansari, R., 2010. Evaluation of nonlocal parameter in the vibrations of single-walled carbon nanotubes with initial strain. Physica E: Low-dimensional Systems and Nanostructures, 42(8), pp.2058-2064.
53. Mazaheri, H., Rahami, H. and Kheyroddin, A., 2018. Static and Dynamic Analysis of Cracked Concrete Beams Using Experimental Study and Finite Element Analysis. Periodica Polytechnica Civil Engineering, 62(2), pp.337-345.
54. Togun, N. and Bağdatlı, S.M., 2016. Non-linear vibration of a nanobeam on a Pasternak elastic medium based on nonlocal Euler-Bernoulli beam theory. Mathematical and Computational Applications, 21(1), p.3.
55. Yokoyama, T., 1987. Vibrations and transient responses of Timoshenko beams resting on elastic mediums. Ingenieur-Archiv, 57(2), pp.81-90.